Ocean Engineering 163 (2018) 40–50

Contents lists available at ScienceDirect

Ocean Engineering

journal homepage: www.elsevier.com/locate/oceaneng

Reliability assessment of point-absorber wave energy converters

Athanasios Kolios[a,*], Loris Francesco Di Maio[a], Lin Wang[b], Lin Cui[c], Qihu Sheng[d]

[a] Offshore Energy Engineering Centre, School of Water, Energy and Environment, Cranfield University, Cranfield, MK43 0AL, UK
[b] School of Mechanical, Aerospace and Automotive Engineering, Coventry University, Coventry, CV1 5FB, UK
[c] National Ocean Technology Centre, Tianjin, 300112, China
[d] Institute of Ocean Renewable Energy System, Harbin Engineering University, Harbin, 150001, China

ARTICLE INFO

Keywords:
Wave energy converters (WECs)
Point-absorber
Reliability analysis
Reliability optimisation
Parametric finite element analysis (FEA)
Response surface modelling

ABSTRACT

Ocean wave energy is a clean and inexhaustible energy resource, capable of providing more than 2 TW of energy supply worldwide. Among all the technologies available to convert wave energy, the point-absorber is one of the most promising solutions today, due to its ease of both fabrication and installation. The floaters of point-absorber WECs (wave energy converters) are generally exposed to harsh marine environments with great uncertainties in environmental loads, which make their reliability assessment quite challenging. In this work, a reliability assessment framework, which combines parametric finite element analysis (FEA) modelling, response surface modelling and reliability analysis, has been developed specifically for the floater of point-absorber WECs. An analytical model of point-absorber WECs is also developed in this work to calculate wave loads and to validate the developed FEA model. After the validation through a series of simulations, the reliability assessment framework has been applied to the NOTC (National Ocean Technology Centre) 10 kW multiple-point-absorber WEC to assess the reliability of the floater, considering the fatigue limit state (FLS). Optimisation of key design components is also performed based on reliability assessment in order to achieve target reliability. The results show that for the considered conditions, the WEC floater is prone to experience fatigue failure before the end of their nominal service life. It is demonstrated that the reliability assessment framework developed in this work is capable of accurately assessing the reliability of WECs and optimising the structure on the basis of reliability.

1. Introduction

Climate change, increasing energy demand globally, rising industrialisation, and population growth rate are just four of the driving factors that constitute clean, sustainable and renewable energy – one of the world's priorities that can enable further development. Although wind and solar energy have attracted significant attention so far, as interaction with natural resources is straightforward, in the last decade more consideration has been given to technologies harvesting energy from waves and tides. Ocean wave energy is a clean and inexhaustible resource, able to provide more than 2 TW of energy supply worldwide (Gunn and Stock-Williams, 2012). Wave energy potential has the advantages of being largely predictable and consistent topologically, as well as having high energy density, making it attractive to coastal countries (Bozzi et al., 2013; Lehmann et al., 2017).

The wave energy sector is today in the pre-commercial phase (Mørk et al., 2010) and much work is ongoing in order to raise the TRL (Technology readiness level) and then reduce the LCOE (Levelized cost of energy) (Salvatore, 2013). The device responsible for capturing and converting wave energy is the wave energy converter (WEC). This technology generally uses a PTO (power take off) system to convert the motion of the floater into electricity to the grid; the floater is one of the key parts of the whole device.

Despite the fact that many different types of WECs have been patented (Drew et al., 2009), only a few of them have been developed and installed at sea (Bozzi et al., 2013). According to the size and direction of elongation, WECs can be roughly categorised into three groups (Drew et al., 2009), i.e. 1) attenuators, in which the principal axis is parallel to the wave propagation direction; 2) terminators, in which the principal axis is perpendicular to the wave propagation direction; and 3) point-absorber, which is insensitive to wave direction due to its small dimensions relative to the incident wavelength.

Among all these different solutions, one of the most promising is the point-absorber technology. First of all, its small dimensions allow the device to be wave-direction independent and capable of absorbing power from all the wave directions, which can be highly varied during the life of the device. Additionally, this technology has the advantages of easy fabrication and installation (Drew et al., 2009; Cretel et al.,

* Corresponding author.
E-mail address: a.kolios@cranfield.ac.uk (A. Kolios).

https://doi.org/10.1016/j.oceaneng.2018.05.048
Received 9 October 2017; Received in revised form 3 April 2018; Accepted 27 May 2018
Available online 04 June 2018

2011). Due to their relatively compact size, the amount of energy that conventional single point-absorber WECs can produce is relatively small when compared to other types of WECs. However, this limitation can be overcome by using multiple point-absorbers, which consist of several floaters.

In a conventional structural analysis, the material properties, environmental loads, model dimensions and parameters are deterministic quantities. This kind of analysis is reliable only in cases where randomness is relatively small. However, modern structures and more specifically those designed for offshore deployment, generally require complex designs, which are more sensitive to uncertainties, considering the environmental, operational and manufacturing processes involved. For such systems, uncertainties in design parameters should be taken into account systematically through stochastic modelling, towards a more realistic and optimised design that would consider the structure's life cycle and associated time-dependent damage mechanisms. Reliability analysis provides an effective approach for better understanding the system response to an input parameter change and hence leads to more reliable designs. In this scenario, this approach to the analysis of the WEC is needed in order to model the uncertainties arising from the high complexity of the model, its material properties, load conditions and PTO characteristics.

The methods used for structural modelling of WECs can be roughly categorised into two groups, i.e. 1) experiments, in which structural responses are measured using sensors such as strain gauges and displacement sensors; 2) FEA (Finite Element Analysis), which predicts structural responses based on numerical simulations. The first method allows the performing of direct experiments in the structure by measuring the strains of the assets considered and then assessing the related stresses. The experimental method has the advantage of being accurate as modelling uncertainty is avoided; however, it is costly and time-consuming when variability of response, due to uncertainty in design variables, is to be considered. The second approach analyses the system response through computer-simulated FEA, allowing for a wide variety of cases to be evaluated. Due to its high flexibility and fidelity, FEA has been widely used for solving complex engineering problems and is extensively applied to the structural modelling of renewable energy devices, such as wind turbine composite blades (Wang et al., 2016a, 2016b, 2016c), offshore support structures (Gentils et al., 2017; Martinez-Luengo et al., 2017) and marine structures (Nicholls-Lee et al., 2011; Tasdemir and Nohut, 2012). Therefore, FEA is chosen in this study for the structural modelling of WECs.

As far as reliability analysis methods are concerned, a series of methods with subsequent variations are available, broadly categorised into analytical and stochastic methods. Common analytical reliability analysis methods are FORM (first order reliability method) (Hohenbichler and Rackwitz, 1982) and the SORM (second order reliability method) (Der Kiureghian et al., 1987) where the limit state function is approached through Taylor's expansions and the problem of evaluating the reliability of a complex system is translated into a problem of mathematical optimisation. SORM performs better in cases of highly non-linear systems, while in other cases, the two methods give similar results (Choi et al., 2006a). With respect to stochastic methods, MCS (Monte Carlo Simulation) (Mooney, 1997) is also commonly applied, mainly due the benefits of direct simulations, hence reducing uncertainty in the results due approximations in the solutions approach, but with the constraint of calculating high probabilities for relatively non-complex engineering systems. For the nature of the problem that this work is investigating, FORM is chosen as the most appropriate method to employ.

Once the reliability assessment of the initial structure is performed for a given stochastic set of inputs, the basis for optimisation of key variables of the model is established. Starting from an initial assessment, it is possible to focus on the parts of the design that go into failure earlier and perform additional analysis to suggest modifications, avoiding failure and achieving the target reliability through a balanced system which avoids unnecessary conservatism.

To the best of the authors' knowledge, the reliability assessment of a point-absorber WEC has not been reported in the literature although reliability has been identified as a key barrier in the further development of ocean energy technologies. This paper aims to develop a reliability assessment framework for point-absorber WEC floaters and then improve the floater's initial design on the basis of reliability. A reliability assessment framework for point-absorber WEC floaters, which combines parametric FEA modelling, response surface modelling and reliability analysis is developed. An analytical model of point-absorber WECs is also developed in this work to calculate wave loads and to validate the FEA model. After the validation through a series of case studies, the reliability assessment framework has been applied to the NOTC (National Ocean Technology Centre) 10 kW multiple-point-absorber WEC to assess its reliability performance.

This paper is structured as follows. Section 2 illustrates the NOTC 10 kW multi-point-absorber WEC. Section 3 presents the analytical model of point-absorber WECs. Section 4 presents the parametric FEA model, and Section 5 details the implementation of the reliability assessment. Results and discussion are presented in Section 6, followed by conclusions in Section 7.

2. NOTC 10 kW multi-point-absorber WEC

The WEC analysed in this study is the NOTC 10 kW multi-point-absorber (see Fig. 1), designed by the NOTC of Tianjin (China) and manufactured by THOECL (Tianjin Haijin Ocean Engineering Corporation Limited). The prototype has six point-absorbers (i.e. floaters) connected to a ship-type platform for the tests. The floaters are cone-shaped and capable of capturing and converting the wave energy through their heave motion. The heave motion of each floater can pump a hydraulic cylinder to produce high pressure oil, which is then transported to the hydraulic motor through pipelines to generate electric power. The overall capacity of the WEC is 10 kW.

Fig. 2a presents the 3D (three-dimensional) geometry model of the whole system, and Fig. 2b depicts a close view of the floater.

3. Analytical model of point-absorber WECs

An analytical model of the point-absorber WECs is developed on the basis of the following assumptions:

- small wave amplitude;
- stable equilibrium of the floater;
- negligible transverse motion of the floater;
- steady-state response in waves.

Fig. 3 shows the schematic of the analytical model of the point-absorber WEC. The bar AD represents the floater arm having an angle θ with respect to the Z axis. Points A and D are pivot points offsetting

Fig. 1. NOTC 10 kW WEC.

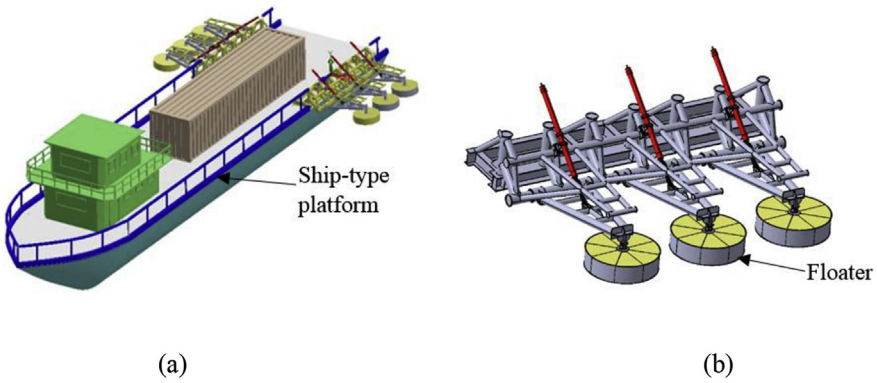

Fig. 2. 3D geometry model: **(a)** whole system, **(b)** close view of the floater.

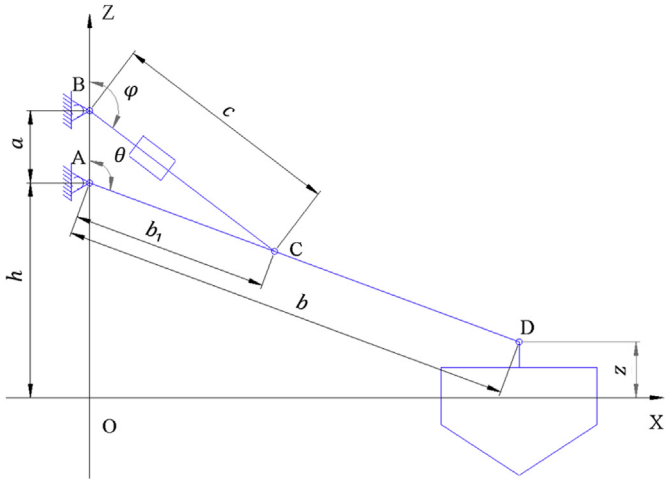

Fig. 3. Analytical model of point-absorber WEC.

from the water surface with a height h and z respectively. The PTO of the system is represented by the bar BC having a length c and an angle ϕ with respect to the Z axis. The lengths of AC and AD are denoted by b_1 and b, respectively.

According to the geometrical relations given in Fig. 3, the length c of the PTO and the top location z of the floater can be respectively expressed as:

$$c = \sqrt{a^2 + b_1^2 - 2ab_1\cos(\theta)} \tag{1}$$

$$z = h - b\sin(\theta) \tag{2}$$

Wave load calculation and kinetic model of the WEC are detailed below.

3.1. Wave load calculation

A wave model of point-absorber WECs has been developed in this work based on the potential flow theory (Lin, 2014), which is a widely used method for calculating wave loads. Considering only the heave motion of the floater, the total force F_3 acting in z-direction can be expressed as:

$$F_3 = \int_{WS} p n_3 dS \tag{3}$$

where p is the linear hydrodynamic pressure at any point of the WS (wet surface) of the floater, n_3 is the vertical component of n, the unit normal direction of the floater surface.

The linear hydrodynamic pressure p in Eq. (3) is given by:

$$p = -\mathrm{Re}\left\{\rho\frac{\partial}{\partial t}(\varphi + \varphi_{in})\right\} \tag{4}$$

where ρ is the seawater density, φ is the perturbation velocity potential, and φ_{in} is the velocity potential of the incident wave.

In case of monochromatic incident waves, the velocity potential φ_{in} can be calculated by:

$$\varphi_{in} = a\,\mathrm{Re}\{\varphi_{in}^0 e^{i\omega t}\} \tag{5}$$

where a is the wave amplitude, ω is the circular frequency, and φ_{in}^0 is the frequency-domain wave potential of a monochromatic wave with unit amplitude.

For infinite depth water level, φ_{in}^0 in Eq. (5) is given by:

$$\varphi_{in}^0 = \frac{g}{\omega}e^{k(z+i\rho)} \tag{6}$$

where k is the wave number and ρ is the function of the direction of the incident waves.

The perturbation velocity potential φ needs to satisfy the following conditions:

$$\nabla^2\varphi = 0 \text{ internal flow field} \tag{7}$$

$$\frac{\partial}{\partial n}\varphi = -\frac{\partial}{\partial n}\varphi_{in} + u_3 n_3 \text{ floater surface boundary condition} \tag{8}$$

$$\frac{\partial^2}{\partial t^2}\varphi + g\frac{\partial}{\partial z}\varphi = 0 \text{ free surface boundary condition} \tag{9}$$

where u_3 is the floater velocity along the vertical direction.

Due to the fact that the perturbation potential of the velocity is linear, it can be decomposed to:

$$\varphi = \mathrm{Re}\{(a\varphi_0 + U_3\varphi_3)e^{i\omega t}\} \tag{10}$$

where φ_0 is the potential of the diffracted waves, φ_3 is the potential of the radiation waves, and U_3 is the amplitude of the velocity. In order to solve these expressions.

Substituting Eqs. (5) and (10) into Eq. (4) yields the pressure p:

$$p = -\mathrm{Re}\left\{\rho\frac{\partial}{\partial t}[(a\varphi_0 + U_3\varphi_3)e^{i\omega t} + a\varphi_{in}^0 e^{i\omega t}]\right\} \tag{11}$$

Substituting Eq. (11) into Eq. (3) gives:

$$F_3 = -a\,\mathrm{Re}\left\{i\rho\omega e^{i\omega t}\int_{WS}(\varphi_0 + \varphi_{in}^0)n_3 dS\right\} + \mathrm{Re}\left\{i\rho\omega U_3\left(\int_{WS}\varphi_3 n_3 dS\right)e^{i\omega t}\right\} \tag{12}$$

Defining the following three coefficients:

$$F_3^0 = -i\rho\omega\int_{WS}(\varphi_0 + \varphi_{in}^0)n_3 dS \tag{13}$$

$$\mu_{33} = -\mathrm{Re}\left\{\rho\left(\int_{WS} \varphi_3 n_3 dS\right)\right\} \tag{14}$$

$$\lambda_{33} = \mathrm{Im}\left\{\rho\omega\left(\int_{WS} \varphi_3 n_3 dS\right)\right\} \tag{15}$$

where F_3^0 is the force coefficient, μ_{33} is the added mass coefficient, and λ_{33} is the damping coefficient.

The final expression for the vertical force is then:

$$F_3 = a\,\mathrm{Re}\{F_3^0 e^{i\omega t}\} - \lambda_{33}\dot{u}_3 - \mu_{33}u_3 \tag{16}$$

Evaluating the coefficients for any reasonable wave frequency allows the estimation of the time dependent force acting on the structure.

3.2. Kinetic model of point-absorber WECs

A kinetic model of point-absorber WECs has been developed in this work based on the law of conservation of energy. The kinetic model aims to assess the energy of all the components of the WEC to evaluate how the forces interact between them, allowing the calculation of the displacement and velocity of the model.

The kinetic energy of the WECs can be expressed as:

$$E = E_1 + E_2 + E_3 + E_4 \tag{17}$$

where E_1 is the kinetic energy coming from the rotation of the floater arm AD around A, E_2 is the kinetic energy coming from the rotation of the hydraulic cylinder and piston BC around B, E_3 is the kinetic energy of the line motion of the hydraulic cylinder and piston, and E_4 is the kinetic energy coming from the heaver motion of the floater.

E_1, E_2, E_3 and E_4 in Eq. (17) can be respectively expressed as:

$$E_1 = \frac{1}{2}J\dot{\theta}^2 \tag{18}$$

$$E_2 = \frac{1}{2}J_p\dot{\phi}^2 \tag{19}$$

$$E_3 = \frac{1}{2}m_p\dot{c}^2 \tag{20}$$

$$E_4 = \frac{1}{2}m\dot{z}^2 \tag{21}$$

where J is the moment of inertia of AD around A, θ is the angle between AD and the z-axis, ϕ is the angle between BC and the z-axis, J_p is the moment of inertia of the PTO around B, m_p is the mass of the PTO, c is length of the PTO, m is the mass of the floater and z is the vertical position of the floater.

Applying the law of conservation of energy to the WEC system gives:

$$\frac{d}{dt}E = [-\rho_w A_w(z - z_0) + a\,\mathrm{Re}\{F_3^0 e^{i\omega t}\} - \lambda_{33}\ddot{z} - \mu_{33}\dot{z}]\dot{z} - [K_p(c - c_0) + \mu_p\dot{c}]\dot{c} \tag{22}$$

where ρ_w is the seawater density, A_w is the water plane area of the floater, F_3^0 is the frequency-domain wave exciting force, λ_{33} is the added mass of the floater, μ_{33} is the damping coefficient, and K_p and μ_p are the stiffness and damping of the PTO, respectively.

$-\rho_w A_w(z - z_0)$ in Eq. (22) is the static restoring force induced by the changing in the draught of the floater. $K_p(c - c_0)$ is the linear restoring force during the PTO movement.

Recalling Eqs. (1) and (2), the following equations can be derived from differentiation:

$$\dot{c} = \frac{ab_1\sin(\theta)}{c}\dot{\theta} \tag{23}$$

$$\ddot{c} = \frac{ab_1\sin(\theta)}{c}\ddot{\theta} + \frac{ab_1\cos(\theta)}{c}\dot{\theta}^2 \tag{24}$$

$$\dot{z} = -[(b_1 + b_2)\sin(\theta)]\dot{\theta} \tag{25}$$

$$\ddot{z} = -[(b_1 + b_2)\sin(\theta)]\ddot{\theta} - [(b_1 + b_2)\cos(\theta)]\dot{\theta}^2 \tag{26}$$

Considering the mass of the PTO is far less than the mass of the moving parts yields:

$$\ddot{\theta} \sim \ddot{\phi} \tag{27}$$

$$\dot{\theta} \sim \dot{\phi} \tag{28}$$

Also introducing:

$$a(\theta) = \frac{ab_1\sin(\theta)}{c} \tag{29}$$

$$a_1(\theta) = \frac{ab_1\cos(\theta)}{c} \tag{30}$$

$$\beta(\theta) = -[(b_1 + b_2)\sin(\theta)] \tag{31}$$

$$\beta_1(\theta) = -[(b_1 + b_2)\cos(\theta)] \tag{32}$$

Substituting Eqs. (17)–(21) and Eqs. (23)–(32) into Eq. (22) gives:

$$\hat{J}\ddot{\theta} + \hat{N}\dot{\theta} + \hat{K}(\theta - \theta_0) = \hat{F} \tag{33}$$

where:

$$\hat{J} = (J + J_p + \alpha^2 m_p + \beta^2(m + \lambda_{33})) \tag{34}$$

$$\hat{N} = \alpha^2\mu_p + \beta^2\mu_{33} \tag{35}$$

$$\hat{K} = \alpha^2\rho A_W + \beta^2 K_p \tag{36}$$

$$\hat{F} = a\,\mathrm{Re}\{F_3^0 e^{i\omega t}\}\beta - \alpha\alpha_1 m_p\dot{\theta}^2 - \left(m + \lambda_{33}\right)\beta\beta_1\dot{\theta}^2 \tag{37}$$

4. Parametric FEA (finite element analysis) model of WEC floaters

A parametric FEA model of WEC floater is developed using the ANSYS software package, a widely used multi-purpose finite element software. The geometry, material, mesh and boundary conditions used in the FEA model are presented below.

4.1. Geometry

The basic design parameters of the WEC floater are provided by the NOTC. The whole system is composed of six cone-shaped floaters having identical dimensions, and therefore only one single floater will be studied in this work. The cone-shaped floater is depicted in Fig. 4.

Three different types of structural reinforcements (stiffeners) are used inside the floater, as depicted in Fig. 5. Further details of dimensions are not disclosed in this paper for confidentiality reasons.

4.2. Material

Different types of steel are used in the fabrication of the NOTC WEC, but for confidentiality reasons they are not disclosed in this paper, as its main purpose is to illustrate the applicability of the methodological framework. In this study, the floater is assumed to be made of S355 steel, which is a typical material used in marine structures. Material properties of S355 steel are listed in Table 1. It should be noted that these properties can also be treated stochastically.

4.3. Mesh

A critical step in the setting up of the model to be used for the FEA is the mesh generation. In order to find the appropriate mesh size, a mesh sensitivity analysis is performed. The ANSYS software package offers a

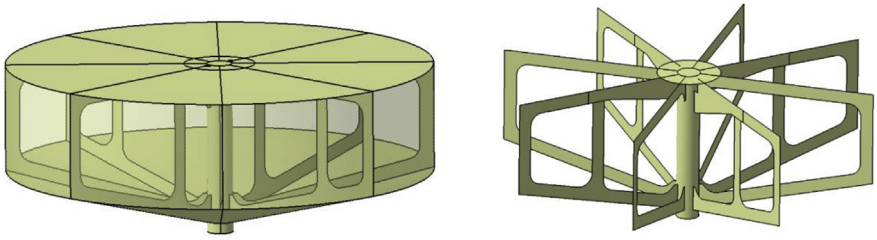

(a) (b)

Fig. 4. Geometry: **a** cone-shaped floater, **b** internal reinforcements of the floater.

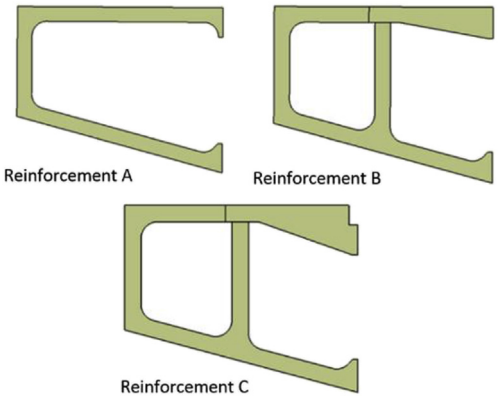

Fig. 5. Structural reinforcements of the floater.

Table 1
Material properties.

Properties	Value
Young's modulus [GPa]	200
Poisson's ratio	0.3
Density [kg/m^3]	7850

reliable and powerful structured mesh generator capable of producing a consistent mesh in all of the structure with low computational requirement – an approach suitable for this study.

Five different mesh sizes were investigated, i.e. 40 mm, 20 mm, 15 mm, 10 mm and 5 mm. In this case, the WEC floater is simulated under the fatigue design load case in China's Bohai area, with a significant wave height of 0.28 m and wave period of 6.2s. The time-dependent wave loads are calculated from the analytical model (see Section 3.1).

Fig. 6 depicts the trend of the maximum von Mises stress with the refining of the mesh size, and detailed mesh analysis data are presented in Table 2.

As can be seen from Fig. 6 and Table 2, the maximum von Mises stress converges at the meshing size of 10 mm, with a relative difference (0.32%) when compared to the further mesh refinement. Therefore, the meshing size of 10 mm is deemed appropriate and thus chosen in this study. The created mesh is depicted in Fig. 7.

4.4. Boundary conditions

In this study two types of boundary conditions are used, i.e. joints and loads. The whole WEC would also include the floater arm but, being outside the scope of this study, it is therefore represented as a beam, as shown in Fig. 8. The relative motion between the adjacent bodies is constrained by revolute joints that constrain three relative displacement DOFs (degrees of freedom) and two out of three relative

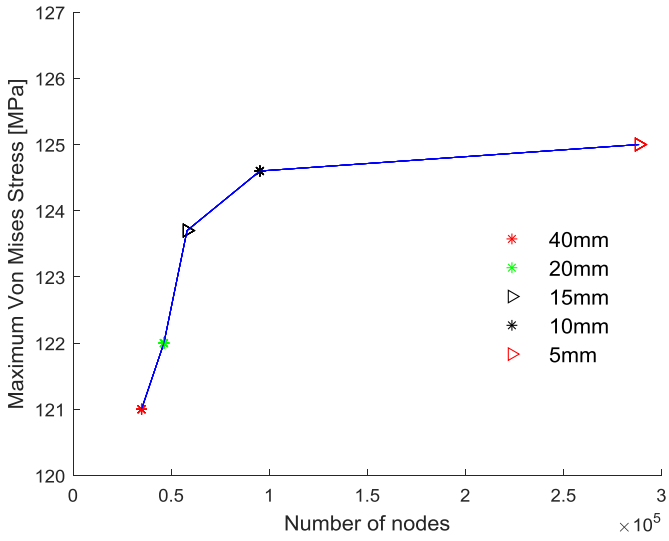

Fig. 6. Calculated maximum von Mises stress.

Table 2
Mesh analysis data.

Element size [mm]	Nodes	Max von Mises Stress [MPa]	Diff [%]
40	34,854	121.0	0.82
20	46,253	122.0	1.37
15	58,050	123.7	0.72
10	95,192	124.6	0.32
5	288,472	125.0	–

rotational DOFs, leaving just one rotational DOF available. To model the PTO of the WEC, a spring joint characterised by PTO stiffness and damping coefficient is also defined. The joints introduced above are also depicted in Fig. 8.

Fig. 9 depicts the load boundary condition used in this study. As can be seen from Fig. 9, the time-dependent wave loads, of which values are obtained from the analytical model presented in Section 3.1, are applied to the floater. The direction of the load can be upwards or downwards depending on the time step considered.

5. Implementation of reliability assessment of WEC floaters

In this section, the reliability assessment of WEC floaters is implemented, considering the fatigue limit state (FLS). The FEA model presented in Section 4 is used to perform stochastic FEA simulations of WEC floaters, taking account of stochastic variables, such as wave loads and material properties. Response surface modelling is then used to post-process the FEA simulation results, deriving the performance function expressed in terms of stochastic variables. Next, FORM is applied to calculate the reliability index, assessing the probability of

(a) (b)

Fig. 7. Mesh: **a** floater, **b** internal structure of floater.

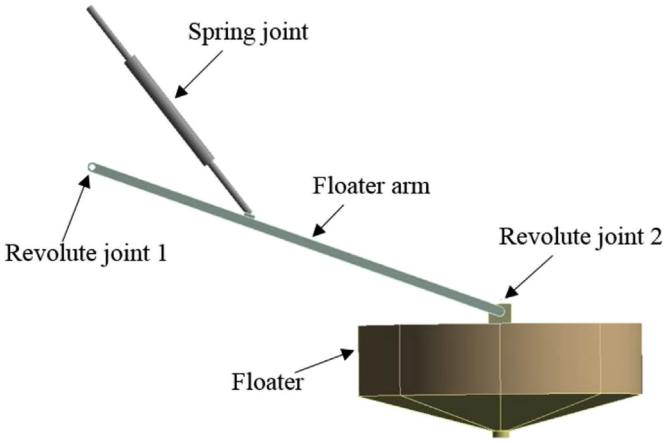

Fig. 8. Joints in the model.

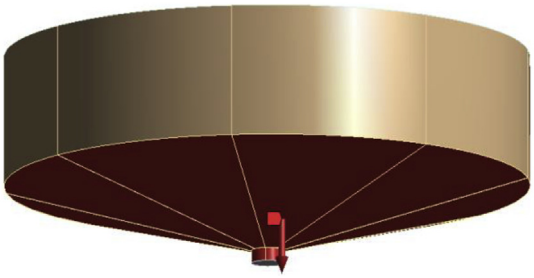

Fig. 9. Load boundary condition.

failure of the structure. The flowchart of the reliability assessment framework is presented in Fig. 10.

5.1. Limit state

As a first step to implement the reliability assessment of a system, the limit states considered have to be defined. The basic design requirement is to give the structure an adequate safety margin that takes into account all the uncertainties in the modelling which affect the integrity of the asset. WECs experience significant cyclic loads induced by the wave, and their design is generally dominated by their fatigue performance. Therefore, the FLS, which evaluates how the structure behaves with repeated load cycles under normal sea condition, is considered in this study.

5.2. Determination of stochastic variables and mapping of the response domain

The main parameters chosen stochastically are generally the ones regarding the load and material properties (resistance) of the structure (Zhang and Zhang, 2013; Zhang and Yang, 2016). In this study, four stochastic variables are considered, i.e. Young's module E, wave load L, spring damping coefficient D and spring stiffness coefficient K, as listed in Table 3; however, the approach can be generalised for a greater number of variables.

In this study, Young's modulus, and the spring's stiffness and damping coefficients are assumed to follow normal distributions (Veritas, 1992). The mean value is the base design condition, while the standard deviation is taken as 15% of the mean in this study. The distribution type, mean and standard deviation of these stochastic

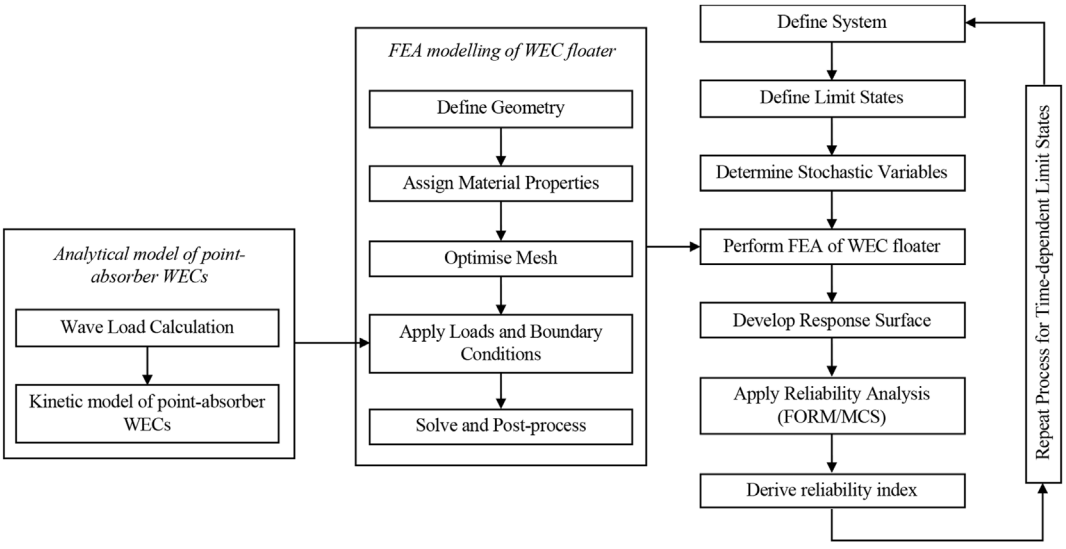

Fig. 10. Flowchart of reliability assessment of WEC floaters.

Table 3
Stochastic variables in the modelling.

Variable	Description
E	Young's modulus
L	Wave load
D	Spring damping coefficient
K	Spring stiffness coefficient

Once the variables are selected, appropriate statistical distributions should be assigned to allow for the reliability analysis.

Table 4
Stochastic parameters.

Variable	Distribution	Mean μ	Standard deviation σ
E [GPa]	Normal	200	30
D [kN/(m/s)]	Normal	320	48
K [kN/m]	Normal	100	15

variables are presented in Table 4.

The wave load is considered differently, based on its dependence on wave height and wave period. To find the peak of the force acting on the system, a truncated Rayleigh distribution (Kolios, 2010) is applied to the wave height allowing the system to consider that, in the case of storm sea conditions, the model can be taken out of the sea to avoid further damage. Once the maximum and minimum wave heights are defined, considering an increment and decrement of 45% from the base load, the Rayleigh distribution is implemented. This distribution is then fitted into a normal-equivalent distribution, to then follow relevant FORM procedures. The latter transformations allow for the extension of the traditional FORM to account for various types of statistical distributions, which can better fit certain variables. In the presence of observed data, distribution fitting algorithms (such as Akaike Information Criterion, Bayesian Information Criterion and Kolmogorov-Smirnov) are often employed to determine the shape coefficients of the most appropriate statistical distributions.

Having defined the stochastic variables, the FEA model presented in Section 4 is then used to perform a series of deterministic FEA simulations of the WEC floater, with the help of the Design of Experiments module and PDS (Probabilistic Design System) in ANSYS, in order to map the response domain and later on derive an appropriate response surface model. This allows the input parameters to be designated as stochastic variables, having different types of distributions. For stochastic simulation, the number of samples is generally chosen between $(2n + 1)$ and 3^n (Kolios, 2010), where n is the number of stochastic variables. The larger number of samples generally enables more accurate results but also requires more computational resources. In order to achieve accurate results, 100 simulations have been performed in ANSYS, which is larger than 3^n, obtaining response values of 100 design samples related to the different stochastic parameters selected. Each parameter is changed by incrementing and decrementing it with $+3\sigma$ and -3σ in order to cover a reasonable and probable range of values. The results are then imported into a MATLAB code that has been developed in this work for response surface modelling, as detailed below.

5.3. Response surface modelling

Response surface modelling is generally used for deriving equation (s) to express a dependent variable in terms of one or more independent variables. Response surface and surrogate modelling methods are two categories of approximation methods that are often employed to model complex engineering systems. The former usually derives analytical expressions of the system (is in the shape of polynomial equations) while the latter stores the system properties normally in a matrix closed-form for further processing. The expressions derived from either category of methods can be further combined with reliability analysis methods, such as FORM/SORM and MCS, as well as employed in multi-disciplinary optimisation problems.

The regression analysis performed in this study is based on the LSM (Least-Square Method) (Choi et al., 2006a), in which the best fit is obtained by minimising the absolute distance between the observed values and the fitted values provided by a fitting model. Its general approach can be expressed as:

$$y(x) = a_0 + a_1 * x_1 + a_2 * x_2 + a_3 * x_3 + ... + a_n * x_n + e \quad (38)$$

where a_i are the regression coefficients and e is the error term in the equation.

Eq. (38) can also be written in the following matrix form:

$$Y = X * A + E \quad (39)$$

where Y is a matrix containing the dependent variables, X is a matrix containing independent variables, A is a matrix with the regression coefficients and E is a matrix with the error terms.

The regression coefficients A can be derived using the LSM:

$$A = (X^T * X)^{-1} * X^T * Y \quad (40)$$

Eq. (38) shows the mathematical expression of a linear regression analysis. In order to achieve a more accurate study, the set of data assessed in this study will be treated with a quadratic regression following the same procedure. Potentially, mixed terms can also be included in the expression to account for the correlation of independent variables at the expense of a higher minimum number of simulations required, but this is not deemed necessary in this case as the variables are sufficiently uncorrelated. As a result, in case of a second-order polynomial with four independent variables, the multivariate polynomial expression can be rewritten as:

$$y(x) = a_0 + a_1 x_1 + a_2 x_1^2 + a_3 x_2 + a_4 x_2^2 + a_5 x_3 + a_6 x_3^2 + a_7 x_4 + a_8 x_4^2 + e \quad (41)$$

5.4. FORM (first order reliability method)

Having obtained the performance function as the expression of safety margin (allowable minus actual/resistance minus load), the FORM is then used to estimate the reliability index through an iterative process. The principle behind this method is based on the fact that the random variables are defined by their first, second moments, and so on. The random variables are transformed in terms of their moments, and the reliability index can be assessed by the approximation of the limit state function.

The probability of failure is computed as:

$$P_f = \Phi(-\beta) \quad (42)$$

where β is the reliability index, also defined as the minimum distance between the MPP (most probable failure point) and the origin, and Φ is the cumulative distribution function of a normal standard variable. Non-normal distributions are accommodated through employing the Hasofer-Lind-Rackwitz-Fiessler method (Choi et al., 2006a), which employs a normalised tail approximation to also account for non-normal distributions. The flowchart of the FORM analysis implemented in the study is based on the FORM presented in Ref. (Choi et al., 2006b).

6. Results and discussion

A generic framework for the reliability assessment for WECs has been developed and reported, and its constituting blocks are validated by a series of case studies. The main components of the reliability assessment framework, i.e. FEA model and FORM, are validated separately. After the validation, the reliability assessment framework has been applied to assess the reliability of WEC floaters and improve the

Table 5
Sea condition.

Item	Values
Mean significant wave height [m]	0.28
Mean wave period [s]	6.2

floater initial design on the basis of reliability.

In this study, the WEC floater is simulated under the fatigue design load in China's Bohai area. The sea condition data are presented in Table 5.

6.1. Validation

Case studies are performed to validate the main components of the reliability assessment framework for WEC floaters, i.e. FEA model and FORM.

6.1.1. Validation of FEA

A case study is performed in order to validate the FEA model. In this case, the wave load is calculated using the method presented in Section 3.1 under the sea condition presented in Table 5. The calculated wave load is then applied to the buoy. In this case, the time step in the FEA model is chosen as 0.138s (corresponding to 1/45 of wave period of 6.2s), which is small enough to ensure good convergence. The vertical displacement and velocity of the buoy calculated from the FEA model presented in Section 4 are compared with the results obtained from the analytical model presented in Section 3.2. The comparison results are depicted in Fig. 11.

From Fig. 11 we can see that 1) both vertical displacement and velocity of the floater vary periodically with the wave load; 2) there is a phase shift between the vertical displacement and velocity; 3) the results from the FEA model show reasonable agreement with those from the analytical model, in terms of both trend and magnitude, with a maximum relative difference of 3% for vertical displacement and of 5% for vertical velocity. The results confirm the validity of both FEA and the analytical model.

6.1.2. Validation of the FORM

For the validation of the FORM, a comparison between the combination of the FORM and RSM, and MCS has been performed for the case of a generic frame structure, as a direct simulation probabilistic assessment of the floater would be computationally unfeasible. The model consists of 40 interconnected members in three levels of the 3D symmetrical geometry with a series of 12 lateral and four vertical loads

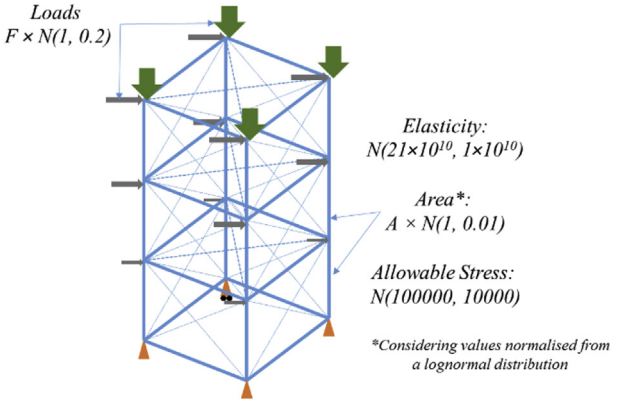

Fig. 12. Reference validation structure and stochastic loads consideration.

applied on the structure. Four stochastic variables are considered, as illustrated in Fig. 12.

For the MCS, a convergence study was performed which concluded that 10^7 simulations were adequate to calculate the joint probabilities for all members; this is also in line with the rule of thumb which suggests for number of simulations an order of magnitude higher than the inverse of the probabilities to be calculated (in this case β values are less than 4.75 which corresponds to a probability of failure of 10^{-6}). From the results presented Fig. 13, it can be seen that there is a trend of FEA/RSM to overestimate reliability index values when compared to direct MCS; however, the difference between predicted values remains consistently below 5%, hence the agreement of the two methods can been considered sufficient. Taking into account that the time required for the FEA/RSM simulations is a few seconds, compared to the MCS, they are considered appropriate for problems similar to the one that is considered in this study.

In a second validation case, the results from the MATLAB FORM code developed in this work are compared against the results from the MCS. The performance function is obtained through post-processing stochastic FEA simulation results through response surface modelling. The comparison results are depicted in Fig. 14 where the MATLAB FORM codes show reasonable agreement with those from MCS (the same approach as mentioned previously for the resolution of the analysis was also followed here), both in terms of trend and magnitude. This further confirms the validity of the MATLAB FORM code developed in this work.

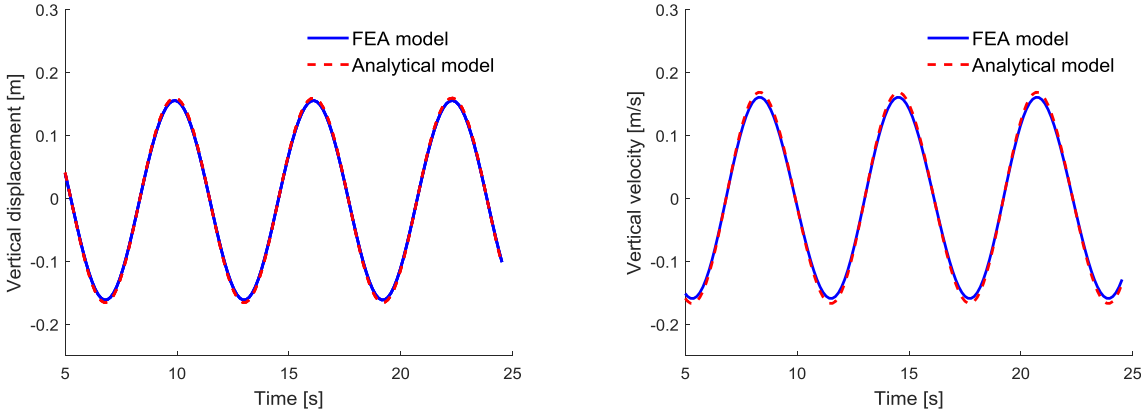

Fig. 11. Comparison of FEA and analytical results: **a** vertical displacement, **b** vertical velocity.

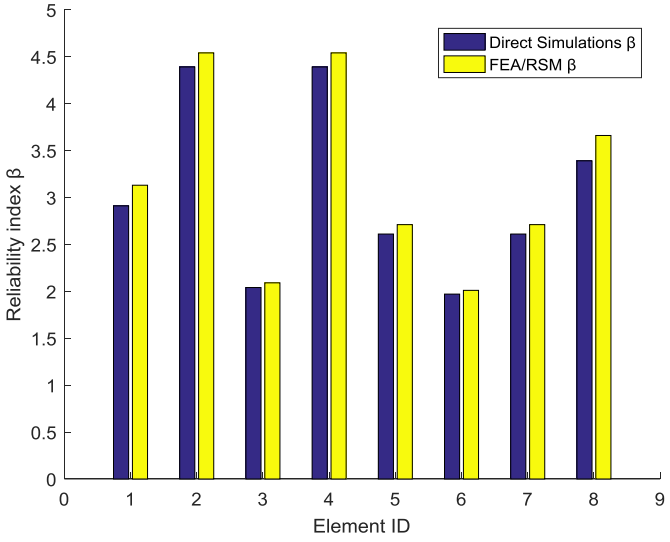

Fig. 13. Stochastic loads consideration for validation case.

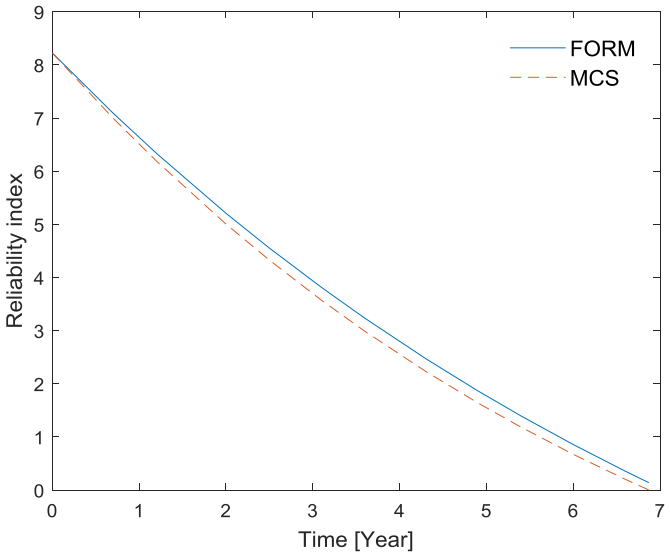

Fig. 14. Reliability index trend.

6.2. Case study application of fatigue based reliability assessment

Following the validation process, the FEA model is further applied to assess the fatigue reliability of the floater and then improve the floater on the basis of reliability.

6.2.1. Fatigue reliability

The fatigue life limit state performed in this study takes into consideration the widely used method of S-N curves. According to this method, the number of cycles to fatigue failure can be assessed by the equation:

$$\log N = A - m \log \Delta S \tag{43}$$

where A is the intercept, m is the slope and ΔS is the equivalent stress range.

Table 6 presents the parameters of the S-N curve used in this study, taken from DNV standard (DNV-RP, 2005).

Reliability index is an important performance parameter, and it is a commonly used probabilistic measure of safety. For fatigue reliability, the reliability index generally varies with time, as the total number of cycles of fatigue loads depends on the length of time. The reliability

Table 6
S-N curve parameters (DNV-RP, 2005).

$N \leq 10^7$		$N > 10^7$	
m	A	m	A
3.0	12.592	5.0	16.320

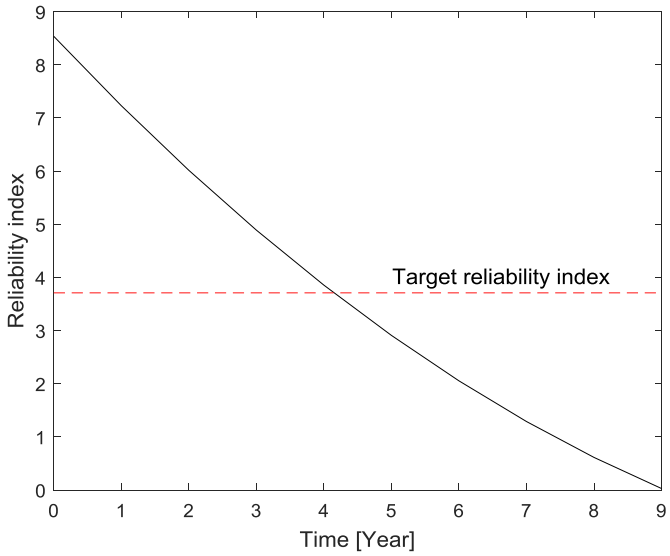

Fig. 15. Reliability index trend.

assessment framework developed in this work is applied to assess the fatigue reliability of WEC floater, calculating the time-dependent reliability index.

The calculated reliability index of the floater under fatigue load case is presented in Fig. 15. As expected, the reliability index reduces as time increases. It can also be observed that the structure does not achieve the reliability target of the 20 years design life (typical value of offshore energy assets), and the reliability index drops below the target reliability index (3.71) after about 4.1 years. This indicates that the design specification considered for this analysis will experience fatigue failure before the end of its target life. The reliability index trend presented in Fig. 15, which is an output of the present reliability assessment framework, provides valuable information for designers regarding how the reliability index reduces with time and if the design achieves the reliability target. If the design does not achieve the reliability target, improvement of the structure on the basis of the reliability is then needed. Further, this predicted performance can inform the operational management strategy of the asset, specifying inspection and predictive maintenance requirements throughout its service life in order to maximise operational availability and reduce downtime.

Additionally, performing all the simulations allows us to understand how the structure behaves in terms of maximum von Mises stress. A local sensitivity analysis can be performed in order to assess what the most critical and important parameters are that can radically change the response and reliability performance of the system. Fig. 16 shows how sensitive to the four design variables the structure is.

As expected, the most critical parameter is the wave force that accounts for 58% of the total sensitivity. Both stiffness and damping coefficients are around 20% and also expected is the fact that the Young's module is only 3%.

6.2.2. Design considerations based on reliability analysis

Starting from the results shown in Section 6.2.1, where reliability values for all components have been calculated, a further study is conducted to improve the behaviour of the structure from a fatigue life perspective. Moreover, considering that the critical point of the system

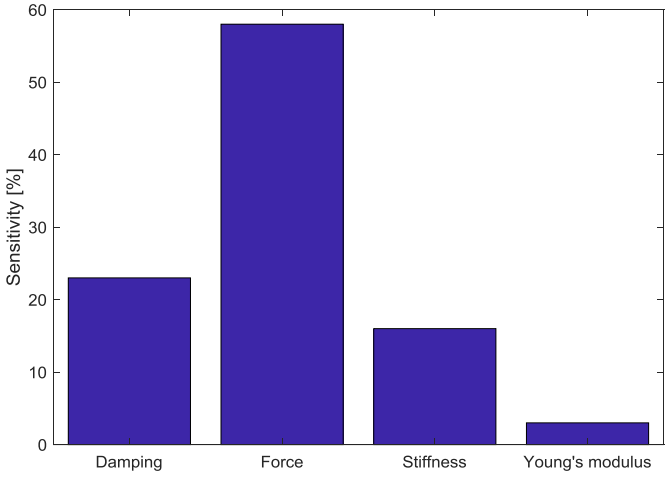

Fig. 16. Local sensitivity factors.

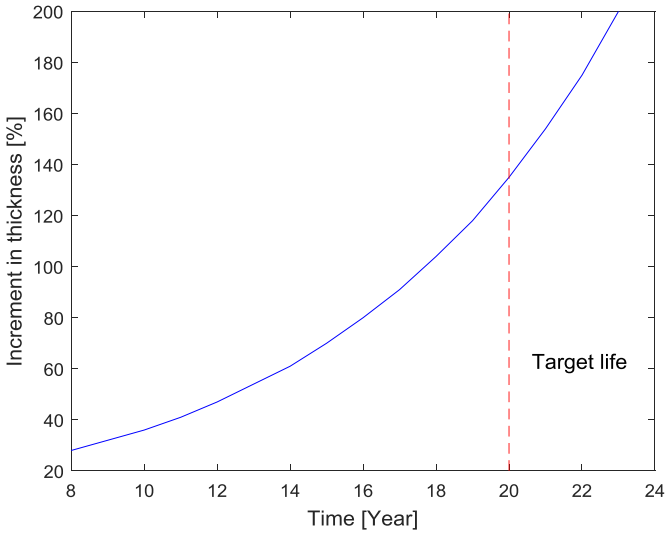

Fig. 17. Optimisation trend with increment in thickness.

is Reinforcement A (see Fig. 5 in Section 4.1) that goes to failure after about 4.1 years, some considerations are made starting from the thickness of this component. In order to achieve the reliability target of 20 years, some changes have to be made in the design. The thickness of Reinforcement A, which is the first one that is expected to fail, is considered as a design variable in this case for refining the design.

A parametric analysis considering different thickness of Reinforcement A is performed, studying the fatigue life of the system with the S-N curve approach. The percentage of increment in the thickness starting from the base load and the design life is represented in Fig. 17.

As can be seen in Fig. 17, the design life of the model increases with the thickness of reinforcement. In this case, the target design life of 20 years is reached at a percentage increment of around 140% in the thickness of Reinforcement A. The practical implication of this result is that the target design life of WEC floaters can be achieved through properly engineering the thickness of the floater structure on the basis of reliability. In this study, fatigue reliability analysis is performed for each incremental thickness of the reinforcement, and the results of reliability analysis are then used to inform improvements to the design in order to achieve target reliability levels. Robustness and efficiency of the method reported herein, allow for a further, more holistic, optimisation approach through appropriate constraints in order to minimise the objective function of mass structure while fulfilling the criterion of target reliability.

It should be noted that the standard deviation of stochastic variables in this study is assumed to be 15% of the mean, which is an assumed value for this case study in absence of more realistic disclosable data. The higher value of standard deviation generally infers to higher scatter in stochastic variables, which results in reduced reliability levels. Detailed investigation on available data for accurate modelling of stochastic variables through experimental tests or structural health monitoring system are highly recommended for detailed design of wave energy converters.

7. Conclusions

In this study, a reliability assessment framework for point-absorber WECs (wave energy converters) has been developed. The framework starts by defining limit states, taking account of the FLS (fatigue limit state). A parametric FEA (finite element analysis) model of point-absorber WECs is developed, considering the stochastic variables (e.g. wave loads and material properties, etc.). The series of FEA simulation results are post-processed through multivariate regression, deriving the performance function expressed in terms of stochastic variables. The FORM (first order reliability method) is then employed to calculate the reliability index and implemented in a MATLAB code. The proposed framework is applied for the reliability assessment of the NOTC (National Ocean Technology Centre) 10 kW multi-point WECs. The following conclusions can be drawn from the present study:

- Both vertical displacement and vertical velocity of the floater calculated from the FEA model show reasonable agreement with those from an analytical model (also developed in this work), which confirms the validity of both FEA and analytical models.
- Good agreement is achieved when comparing the reliability index calculated from the MATLAB FORM code against those from literature and MCS (Monte Carlo simulation), which confirms the validity of the MATLAB FORM code developed in this work.
- The reliability index of the floater under the FLS drops below the target reliability index (3.71) after about 4.1 years, which indicates the floater is likely to experience fatigue failure.
- To reach the target life of 20 years some decisions regarding the thickness and design of the structure have to be made.
- In the considered case study, increasing the thickness of the reinforcement by around 140% results in the floater achieving the reliability target levels.

Based on the evidence presented in this paper, the reliability assessment framework developed and reported in this work is capable of accurately assessing the reliability of point-absorber WECs and setting the basis for improving the design of the structure on the basis of reliability. The methodology can be further applied in similar problems of ocean energy technologies where complex systems are subject to a variety of uncertain design variables.

Acknowledgements

This work was supported by grant EP/M020339/1 for Cranfield University, from the UK Engineering and Physical Sciences Research Council.

References

Bozzi, S., Miquel, A.M., Antonini, A., Passoni, G., Archetti, R., 2013. Modeling of a point absorber for energy conversion in Italian seas. Energies 6 (6), 3033–3051.
Choi, S.-K., Grandhi, R.V., Canfield, R.A., 2006a. Reliability-based Structural Design. Springer Science & Business Media.
Choi, S.-K., Grandhi, R., Canfield, R.A., 2006b. Reliability-based Structural Design. Springer Science & Business Media.
Cretel, J.A., Lightbody, G., Thomas, G.P., Lewis, A.W., 2011. Maximisation of energy

capture by a wave-energy point absorber using model predictive control. IFAC Proc. Volumes 44 (1), 3714–3721.
Der Kiureghian, A., Lin, H.-Z., Hwang, S.-J., 1987. Second-order reliability approximations. J. Eng. Mech. 113 (8), 1208–1225.
DNV-RP, D., 2005. C203 fatigue design of offshore steel structures. Recomm Pract DNV-RPC203 126.
Drew, B., Plummer, A.R., Sahinkaya, M.N., 2009. A Review of Wave Energy Converter Technology. Sage Publications Sage UK, London, England.
Gentils, T., Wang, L., Kolios, A., 2017. Integrated structural optimisation of offshore wind turbine support structures based on finite element analysis and genetic algorithm. Appl. Energy 199, 187–204.
Gunn, K., Stock-Williams, C., 2012. Quantifying the global wave power resource. Renew. Energy 44, 296–304.
Hohenbichler, M., Rackwitz, R., 1982. First-order concepts in system reliability. Struct. Saf. 1 (3), 177–188.
Kolios, A., 2010. A Multi-configuration Approach to Reliability Based Structural Integrity Assessment for Ultimate Strength.
Lehmann, M., Karimpour, F., Goudey, C.A., Jacobson, P.T., Alam, M.-R., 2017. Ocean wave energy in the United States: current status and future perspectives. Renew. Sustain. Energy Rev. 74, 1300–1313. ISSN: 1364-0321. https://doi.org/10.1016/j.rser.2016.11.101.
Lin, P., 2014. Numerical Modeling of Water Waves. CRC Press.
Martinez-Luengo, M., Kolios, A., Wang, L., 2017. Parametric FEA modelling of offshore wind turbine support structures: towards scaling-up and CAPEX reduction. Int. J. Marine Energy 19, 16–31. ISSN 2214-1669. https://doi.org/10.1016/j.ijome.2017.05.005.
Mooney, C.Z., 1997. Monte Carlo Simulation. Sage Publications.
Mørk, G., Barstow, S., Kabuth, A., Pontes, M.T., 2010. Assessing the global wave energy potential. In: Proc. Of 29th International Conference on Ocean, Offshore and Arctic Engineering, ASME, Paper.
Nicholls-Lee, R., Turnock, S., Boyd, S., 2011. A Method for Analysing Fluid Structure Interactions on a Horizontal axis Tidal Turbine.
Salvatore, J., 2013. World Energy Perspective: Cost of Energy Technologies. World Energy Council.
Tasdemir, A., Nohut, S., 2012. Fatigue analysis of ship structures with hinged deck design by finite element method. A case study: fatigue analysis of the primary supporting members of 4900 PCTC. Mar. Struct. 25 (1), 1–12.
Veritas, N., 1992. Structural Reliability Analysis of marine Structures. Det Norske Veritas.
Wang, L., Kolios, A., Nishino, T., Delafin, P.-L., Bird, T., 2016a. Structural optimisation of vertical-axis wind turbine composite blades based on finite element analysis and genetic algorithm. Compos. Struct. 153, 123–138.
Wang, L., Quant, R., Kolios, A., 2016b. Fluid structure interaction modelling of horizontal-axis wind turbine blades based on CFD and FEA. J. Wind Eng. Ind. Aerod. 158, 11–25.
Wang, L., Liu, X., Kolios, A., 2016c. State of the art in the aeroelasticity of wind turbine blades: aeroelastic modelling. Renew. Sustain. Energy Rev. 64, 195–210.
Zhang, Y., Yang, Z., 2016. Reliability sensitivity numerical analysis of mechanical structure based on gamma processes. Adv. Mech. Eng. 8 (12) 1687814016679624.
Zhang, Y., Zhang, Y., 2013. A new stochastic analysis method for mechanical components. Proc. IME C J. Mech. Eng. Sci. 227 (8), 1818–1829.